

Damage of scarf-repaired composite laminates subjected to low-velocity impacts

Xiaoquan Cheng ^{*1}, Wenyi Zhao ^{1a}, Shufeng Liu ^{1b}, Yunyan Xu ^{1c} and Jianwen Bao ^{2d}

¹ School of Aeronautical Science and Engineering, Beihang University, Beijing 100191, China

² Beijing Institute of Aeronautical Materials, Beijing 100095, China

(Received February 02, 2014, Revised July 28, 2014, Accepted August 04, 2014)

Abstract. The damage characters of scarf repaired composite laminates subjected to low-velocity impact with various energy levels at different locations are studied experimentally. The results are compared with those of the original laminates which have no initial damage and don't need repair. The impact load-time history of the specimens, the velocity-time curves of the impactor, the post impact compressive strength of the specimens and the C-scan photographs of the damaged regions are obtained. The delamination threshold load and damage character of the specimen section at impact point are also studied. The results have shown that the impact response of a repaired composite laminate is sensitive to the location of the impact. The impact load and the delamination threshold load have shown different characters for specimens with different impact locations. The debonding characters of the adhesive and compressive strength after impact of the specimens are also influenced by impact locations.

Keywords: composite laminates; scarf-repair; low-velocity impact; damage; compressive strength

1. Introduction

Laminated composite structures are extensively used in aerospace flight vehicle structures due to composite materials with high specific modulus and high specific strength. The panel skin structures of modern airplanes are almost made of composite laminates, where the damage cannot be avoided, particularly low-velocity impact damage from outer objects. The repair techniques of composite structures have received more attention for they are usually cheaper than replacement of the whole parts. There are mainly two repair methods for composite structures: bolted repair and bonded repair. Scarf repair, which is categorized as bonded repair, is more advanced for keeping the aerodynamic shape of airplanes and achieving a better recovery of strength and stiffness. Therefore, scarf repair has a promising prospect in aviation industry and is the hot spot of current

*Corresponding author, Professor, Ph.D., E-mail: xiaoquan_cheng@buaa.edu.cn

^a Ms.D. Student, E-mail: my_reality@163.com

^b Ph.D. Student, E-mail: liufeng_9760@126.com

^c Ph.D. Student, E-mail: [bxhuyunyan@sina.com](mailto:bhxuyunyan@sina.com)

^d Ph.D. Professor, E-mail: baojianwen@hotmail.com

researches on composite structure repair.

Considerable studies in the past decades have enabled the development in design tools and application methodologies of scarf repair for fiber reinforced composites structures (Baker 1999, Falzon 2009, Harman 2006, Wang and Gunnion 2008). Previous work has revealed the influences of scarf angle, adhesive thickness and ply sequences on the bearing capacity of the scarf-repaired laminates, and has suggested a scarf angle of 6° and adhesive thickness of 0.15–0.25 mm to be an optimal choice, considering both repair efficiency and operation viability (Baker 1999, Harman 2006). Harman (2006) showed that if the adhesive modulus is mismatched, a stress concentration which is proportional to the degree of mismatch will form near the tip of the scarf joint. Wang and Gunnion (2008) discovered that significant adhesive stress concentration exists at the terminations of the stiffer plies along the joint, which results in reducing the joint strength, particularly in room temperature dry conditions. Kumar *et al.* (2005, 2006) also elaborated the failure mechanism of scarf-repaired laminates under compressive and tensile loads.

Except for the conventional tensile and compressive load carrying abilities, the repaired structures are inevitably faced with the threat of impact damages, since impacts may occur during manufacture and normal operations of maintenance.

Numerous analytical and numerical methods have been established to predict the damage evolution in original composite laminates subjected to low velocity impact (Abrate 1991, 1994). And there are also a lot of studies on compressive strength after low-velocity impact (CAI strength) of intact laminates, composite honeycomb sandwich panels and stitched laminates (Cheng *et al.* 1998, 2002, 2009). But little attention has been paid to the damage tolerance of the repaired composite structures, particularly the low-velocity impact damage.

Takahashi *et al.* (2007) established a damage detecting system for scarf-repaired laminates subjected to low velocity impact. The results indicated that the debonding at the interface between the adhesive layer and the repair laminates was caused by the shear cracks and delaminations near the impact point and propagated towards the bottom surface. And the effects of impact energy on the debonding boundary were also studied. Hoshi *et al.* (2007) has investigated the impact characteristics of CFRP scarf joint and it was found that the impact damage increased with the increase of scarf angle and the residual strength of scarf joint decreased when scarf angle and impact energy increased. The presence of scarf joint reduces the damage tolerance of the parent structures through introduction of a tapered tip which is vulnerable to low velocity impact. Some numerical methods were proposed to investigate the damage tolerance and impact resistance of scarf joint (Harman and Wang 2007, Herszberg *et al.* 2007). Harman and Rider (2011) assessed the relative reduction of both tension and compression strength caused by a low energy impact to original composite structures and to repaired structures in the region of high damage sensitivity. And the effects of hygrothermal environment condition on the CAI strength and tensile strength after impact (TAI strength) on the scarf-repaired laminates were also studied, which indicated that CAI strength is more vulnerable to hygrothermal environment condition than TAI strength.

However, the researches above are all about 2D scarf joint, which cannot be used in the practical engineering. Usually, 3D scarf joint is used to repair composite structures. Due to the complexity of the configuration in 3D scarf-repaired laminates, impact in different locations will make big differences in damage propagation. This paper presents an experimental study on 3D scarf-repaired CCF300/5228A laminates subjected to low velocity impact at different locations. The impact load, delamination threshold loads (DTLs), CAI strength and ultrasonic C-scan photographs have all been obtained through experimental tests and the influence of impact locations on the load response, DTLs and CAI strengths is also analyzed.

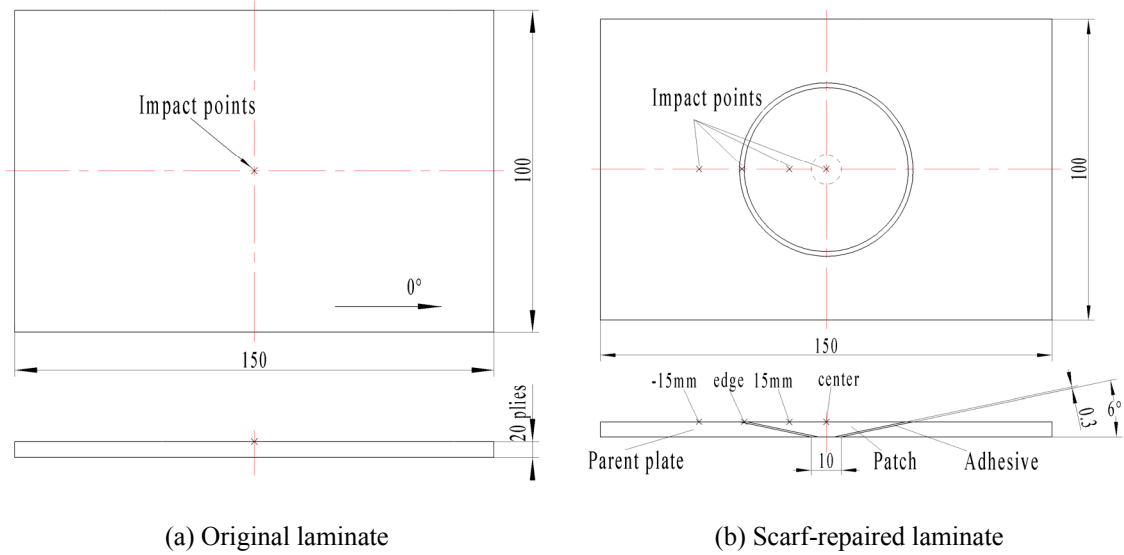


Fig. 1 Low-velocity impacted specimen configurations

Table 1 Test matrix

Specimen	Impact location	Specimen group	Impact energy	Specimen number
Original laminates	P1	Group 1	1.55 J	1
			4.61 J	1
			4.45 J/mm	2
			6.67 J/mm	3
Scarfed-repaired laminates	P2	Group 2	1.55 J	1
			4.61 J	1
			4.45 J/mm	2
			6.67 J/mm	3
Scarfed-repaired laminates	P3	Group 3	1.55 J	1
			4.61 J	1
			4.45 J/mm	2
			6.67 J/mm	4
Scarfed-repaired laminates	P4	Group 4	1.55 J	1
			4.61 J	1
			4.45 J/mm	2
			6.67 J/mm	4
Scarfed-repaired laminates	P5	Group 5	1.55 J	1
			4.61 J	1
			6.67 J/mm	3

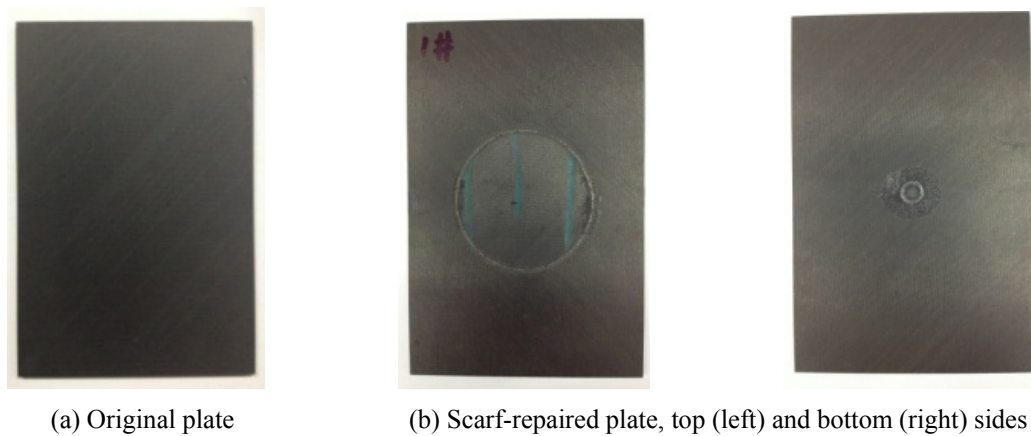


Fig. 2 Photographs of specimens

2. Specimens

2.1 Specimen design

There are two kinds of specimens in this study, including the original laminated specimens and the scarf-repaired laminated specimens. Both of them are of the same size which is 150 mm in length and 100 mm in width. The 0° direction is parallel to the long sides. Bottom diameter of scarf-repair region is 10 mm, and the scarf angle is 6° . Schematic diagrams of the specimens can be found in Fig. 1.

Low-velocity impacts in different energy levels are proposed in geometric center (location P1) of original plates and in four locations of scarf-repaired plates separately. The impact points are all aligned on the width center line for both kinds of specimens. For repaired specimens, the specific locations of impact points are at the patch center (location P2), the middle of adhesive area (location P3), the edge of the patch (location P4) and outside the patch (location P5), as is shown in Fig. 1(b). Table 1 gives the contents of experimental work contained here.

2.2 Specimen manufacture

Carbon fiber reinforced epoxy CCF300 / 5228A is chosen as the material of the specimens, for it is cheap and has been frequently used in airplane structures. Its properties have been acquired by abundant experiments. The specimens are manufactured through autoclave modeling. SY-14M is chosen as the material of the adhesive, its thickness is about 0.13 mm in the repaired plates.

While designing the specimens, some commonly used stacking sequences in airplane skins are taken as reference. The specimens are finally designed as 20 ply graphite/epoxy laminates with the stacking sequence of $[45/0_2/-45/90/45/0_2/-45/0]$ s, where 0° plies account for 50%, $\pm 45^\circ$ plies account for 40% and 90° plies account for 10%.

The material and stacking sequence of the patches, which are processed from completely cured laminates by a Computer Numerical Control (CNC) machine, exactly coincide with those of the parent plates. A conical frustum shaped groove is milled in the original plate by the CNC milling

machine as the parent plate of the repaired specimen. The patch, the parent plate and the adhesive film are then fixed together and placed in an environmental chamber for secondary curing. Photographs of original and repaired laminate specimens are shown in Fig. 2.

3. Experiment method

Low-velocity impact test is conducted on a dual-rail drop-weight impact test machine. Specimens are fixed to the impact support fixture with four point clamps according ASTM D7136 / D7136M-07. The impactor weighs 5.5 kg, which punch has a steel hemisphere surface with a diameter of 12.7 mm. The impacting axis is perpendicular to the plane of the specimen and the energy and velocity of impact can be controlled by adjusting the height of the impactor. A KISTLER 9331B dynamic load sensor is installed between the mass and the punch in order to record the contact load history during impact.

Generally, damages of composite laminates under low-velocity impact will expand internally. It can be observed in the back surface of the specimen in forms of fiber breakage, local buckling, etc. C-scan, color photographs and the cross-sectional optical microscopy imaging techniques are used to observe the impact damage condition.

A pulse echo C-scan is conducted on each of the impact damaged specimens. In order to calculate the damage area, the digitized scan images are imported into Adobe Photoshop, so that the number of pixels within the damaged region could be counted. As the edge lengths of the specimens are already known, the dimension of each pixel can be easily derived, and the areas of the damage zone can be determined subsequently.

In order to further characterize the damage, some of the coupons are sectioned through the center of the damage area and then taken to the microscopic examination. The cut pieces are mounted in one-inch diameter cups of potting resin with the edges of interest forming a coincident face to enable fine polishing. The specimens are then polished so as to produce a scratch free surface with a tolerance of less than three micron, which allows visibility of the intra-ply damage.

Compression tests after impact are performed on the INSTRON 8803 hydraulic material testing machine. According to standard ASTM D7137/D7137M-07, the specimens are clamped in a fixture so that the load would be uniform and failure would occur in the test section. The loading speed is 1.25 mm/min.

4. Low-velocity impact responses of laminates

4.1 Impact with low energy level

When subjected to a low-velocity impact, the permanent damage of the specimens does not occur in a certain energy range. Instead, the impact force triggers elastic bending and vibration of the specimens, accompanied with energy absorption and slight matrix cracking.

The contact load-time history of original laminate specimens subjected to a 1.55 J impact is shown in Fig. 3. The load curve contains some minor oscillations due to vibration and elastic wave responses of the specimen. This phenomenon is repeatable, as described in a previous study (Cheng *et al.* 1998). There is no visible indent on the impacted surface, and no visible cracks or other signs of damage on the back surface either.

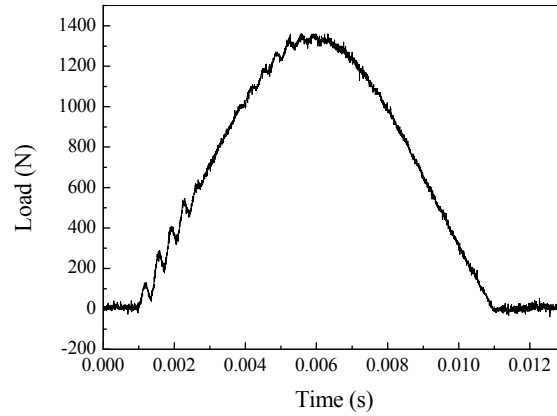


Fig. 3 Contact load history of original plate subjected to 1.55 J impact

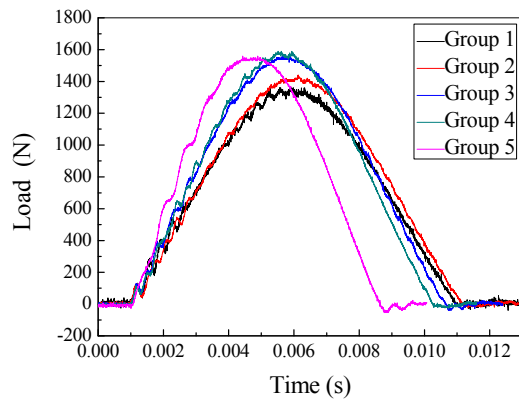


Fig. 4 Contact load history of five group specimens subjected to 1.55 J impact

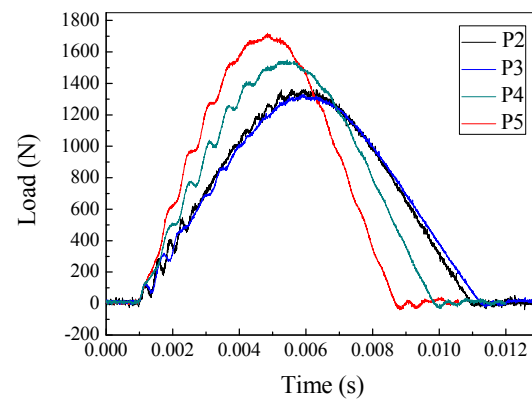


Fig. 5 Contact load history of original plates subjected to 1.55 J impact at 4 different locations

As shown in the figure, the shape of the load-time curve is close to that of half a sine curve, and the response load history can be accurately simulated with a single-degree-of-freedom system as the following equation (Harman and Rider 2011).

$$F = V\sqrt{KM} \sin\sqrt{K/M}t \quad (1)$$

where K is the stiffness of the laminate, M is the mass of the impactor, and V is the initial velocity of the impactor.

Fig. 4 shows the load histories of all the five group specimens subjected to 1.55 J impact. The curves show that the wavelength and amplitude of Group 1 and Group 2 are close to each other. The wavelength of Group 3 and Group 4 is less than that of Group 1. The wavelength of Group 5 has significantly decreased comparing to the other groups, while the amplitude is similar to those of Group 3 and Group 4.

In the tests, variables M and V of Eq. (1) have both stayed constant. Hence, the differences

among the shapes of the curves must have been resulted from the diversified values of K , named the stiffness of the laminates.

In order to find out whether the variety of the equivalent stiffness is induced by relative position between the patch and the impact location, or by the varying distances between the punch and the impact fixture support edges, a set of comparative tests are performed. In these tests, a 1.55 J impact is imposed on original laminates at four different locations corresponding to P2, P3, P4 and P5 of the repaired laminates. The load-time curves are shown in Fig. 5.

In Fig. 5, the curves which represent for specimens impacted at the location of P2 and P3 almost coincidence with each other. The other two curves have evident differences in wavelength and amplitude, which can be derived from the variety of equivalent stiffness with reference to Eq. (1). Since the influence of the relative position between the impact point and the patch has been eliminated, the variety of equivalent stiffness must be triggered by the varying distances between the punch and the impact fixture.

When it comes to 4.61 J impact, the existence of DTL can be easily determined from the response load.

The load-time history for original laminate specimen subjected to a 4.61 J impact is shown in Fig. 6. It can be seen that the loads drop suddenly and sharply after reaching a certain value, and oscillations exist in the entire contact process for all groups of specimens. The sudden load drop is the result of the instable expansion of interlaminar damage. This is an obvious difference from the result of 1.55 J impact. There is no such load drop in the latter ones.

For a certain kind of specimen, the DTL varies from one impact energy level to another. As long as the peak load is slightly higher than the DTL, the DTL can be distinguished from load history curves. The DTL of all specimen subjected to 4.61 J impact is shown in Table 2.

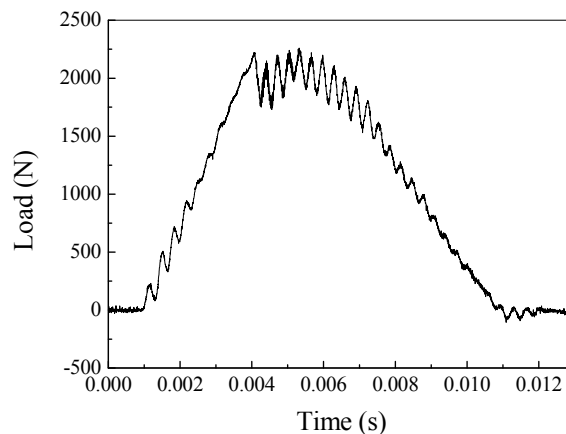


Fig. 6 Contact Load histories of original laminate specimen to 4.61 J impact

Table 2 DTL for five group of specimen subjected to 4.61 J impact

Specimen	Group 1	Group 2	Group 3	Group 4	Group 5
DTL (kN)	2.22	1.93	2.18	2.41	2.61

4.2 6.67 J/mm impact

Fig. 7(a) shows the load and velocity history curves for a specimen in Group 1 subjected to 6.67 J/mm impact. In the beginning portion of the curve, load fluctuates across several small peaks, then rises to relatively large oscillations. After the maximum impact load, the load plunges into severe oscillating region. Afterwards, the load gradually reduces to 0. According to the velocity history curve, during the velocity decrease, the punch has reached the maximum displacement before it starts to rebound. The 'Z point' in the figure represents for the rebound point where the punch velocity is zero. It is corresponding to the 'R point' in the load history curve, which indicates that the load curve following the 'R point' reflects an unloading process.

The load-time curve of a specimen in Group 2 subjected to 6.67 J/mm impact is shown in Fig. 7(b).

The DTL can be easily determined from the figure. After onset of the delamination, the response load increases in oscillations and reaches a higher level in a manner similar to quadric function, then decreases to zero gradually.

The load-time curve of a specimen in Group 3 subjected to 6.67J/mm impact is shown in Fig. 7(c).

The response load increases from zero to DTL through several slight oscillations, then begins to increase with severe ones, and forms a platform around a higher load. After that, the load decreases to zero smoothly.

The load-time curve of a specimen in Group 4 subjected to 6.67 J/mm impact is shown in Fig. 7(d).

The impact response load increases from zero to DTL in a nearly smooth way, with little oscillations in the procedure. After reaching DTL, the response load starts to oscillate intensively without significant increase in the peak load. Thus, the maximum impact response load is close to DTL in this case. After that, the response load decreases to zero smoothly.

The load-time curve of a specimen in Group 5 subjected to 6.67 J/mm impact is shown in Fig. 7(e).

The impact response load increases from zero to DTL smoothly with little oscillations, then starts to oscillate violently with increasing amplitudes. The load begins to decrease after maximum load point. There seems to be a second oscillation region during the decrease. There is no sudden load drop after reaching the maximum response load, compared with the original plates subjected to the same loading condition.

4.3 4.45 J/mm impact

The load-time curves of the Group 1 and Group 4 specimens subjected to 4.45 J/mm impact are shown in Fig. 8 respectively.

The impact response load of the original plates drops sharply after reaching DTL, then increases to the maximum load and drops sharply again. Afterwards, the load shows trend of second oscillation and decreases to zero subsequently.

For the scarf repaired plates, impact at P2 and P3 have triggered similar trends of the curves. In these both cases, the load drops slightly at DTL, then increases and forms a raised platform similar to a quadric function on the load-time curve before it decreases to zero. The oscillations are more violent when impact at P3, while the curves are smoother when impact at P2. For the specimens impacted at P4, their load-time curves almost degenerate into platforms with intensive oscillations

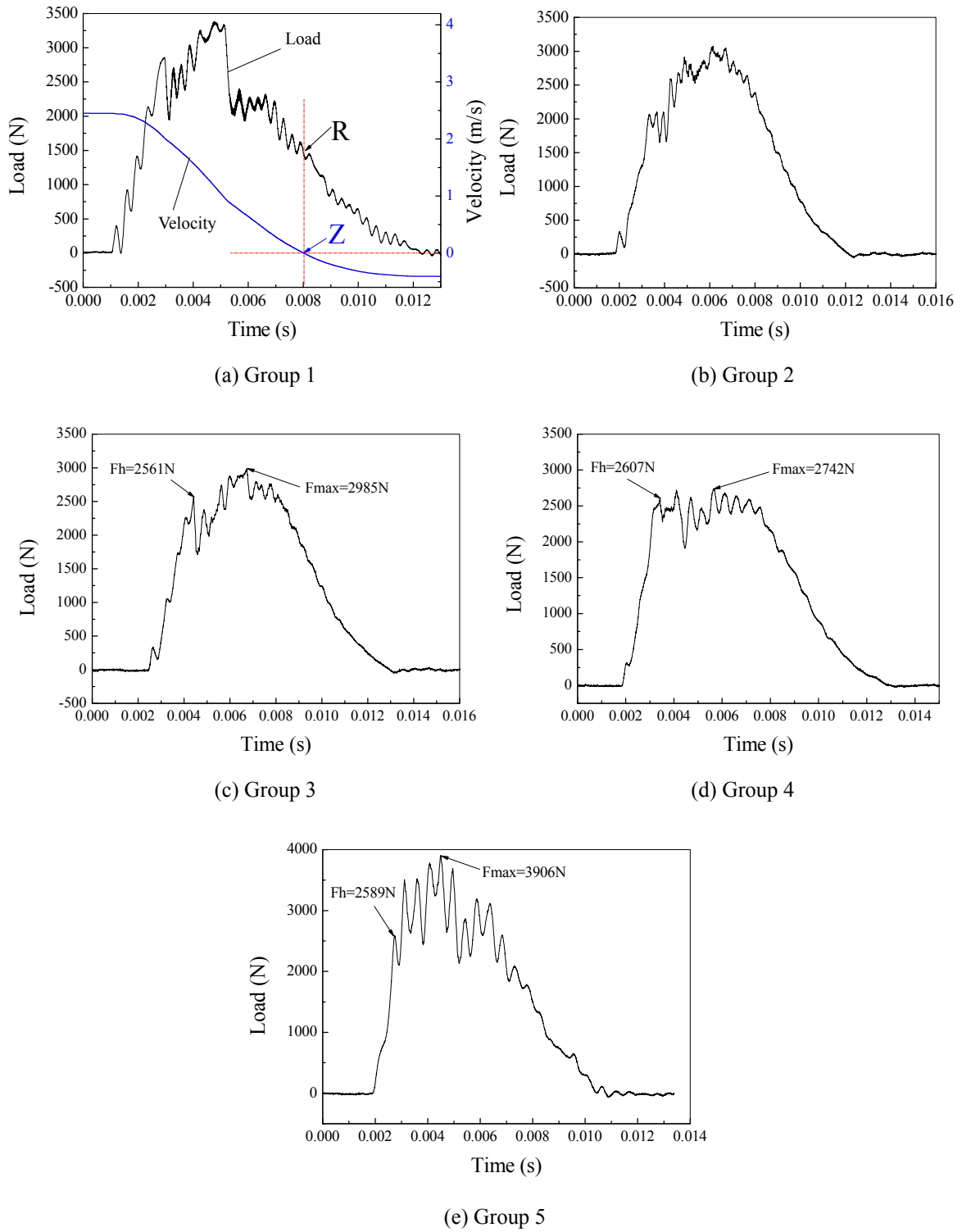


Fig. 7 Load history curves of five group specimens subjected to 6.67 J/mm impact

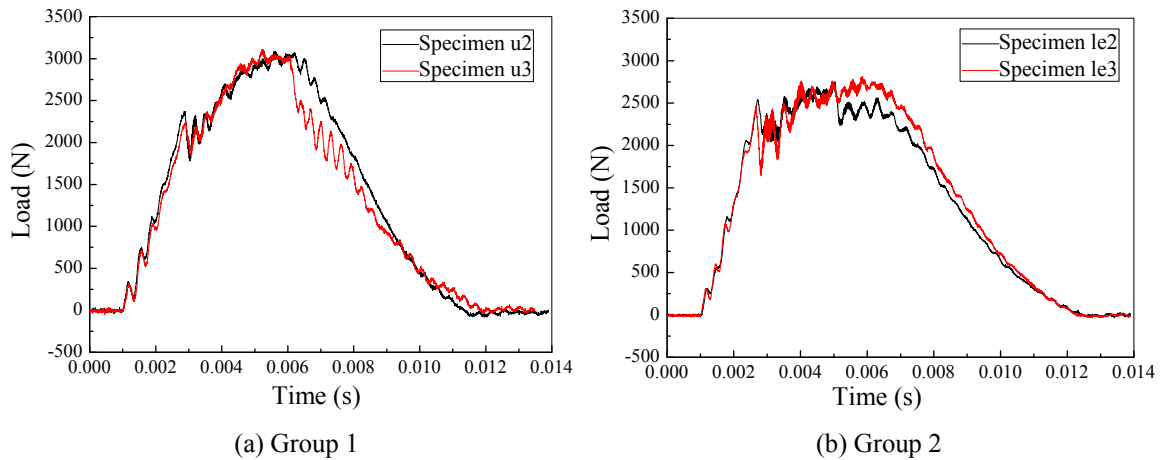


Fig. 8 Load histories of specimens subjected to 4.45 J/mm impact

occur after DTL. There is no significant increase of the response load afterwards. Comparing with the other three groups, impact at P5 has resulted in the highest DTL and the lowest maximum impact load.

4.4 Comparative analysis

Comparing load-time curves of specimens subjected to 4.45 J/mm (see Fig. 8) with 6.67 J/mm (see Fig. 7) impact, it can be found that the damage propagation of scarf repaired composite laminates differs from original laminates. For scarf repaired laminates, the impact position also exists specific influence on the damage propagation.

Firstly, there is less oscillations before DTL. Secondly, the impact at P2 and P3 has triggered similar responses. Thirdly, when impact at P4, the load-time curve degenerates into a platform, the peak load is close to the DTL while the peak load during the impact is lower than all other cases in this study. Fourthly, when impact at P5, the impact response is similar to that of an original plate, but a higher maximum load and shorter impact duration is generated on a repaired laminate.

For low-velocity impact with the energy of 4.61 J, 4.45 J/mm and 6.67 J/mm, DTL can be determined directly from the load-time curves. The results are shown in Fig. 9.

The DTL of 4.61J impact is shown in Fig. 9(a). There is no scatter marked in this figure since there is only one specimen for each impact location. Fig. 9(b) regards to the DTL of 4.45 J/mm impact. There are two specimens for each impact location. Fig. 9(c) regards to the DTL of 6.67 J/mm impact. There are 3 or 4 specimens for each impact location. The figures have shown that DTL of original laminates impacted at P1 and repaired laminates impacted at P2 are close to each other. For repaired laminates subjected to impact of the same energy level, DTL increases slightly when the impact position moves outwards from the center (from P2 to P5).

When subjected to a higher energy impact (6.67 J/mm), a higher scatter of DTL is gained. Nevertheless, the result still implicates that a lower DTL can be gained when the repaired laminate is impacted at P2.

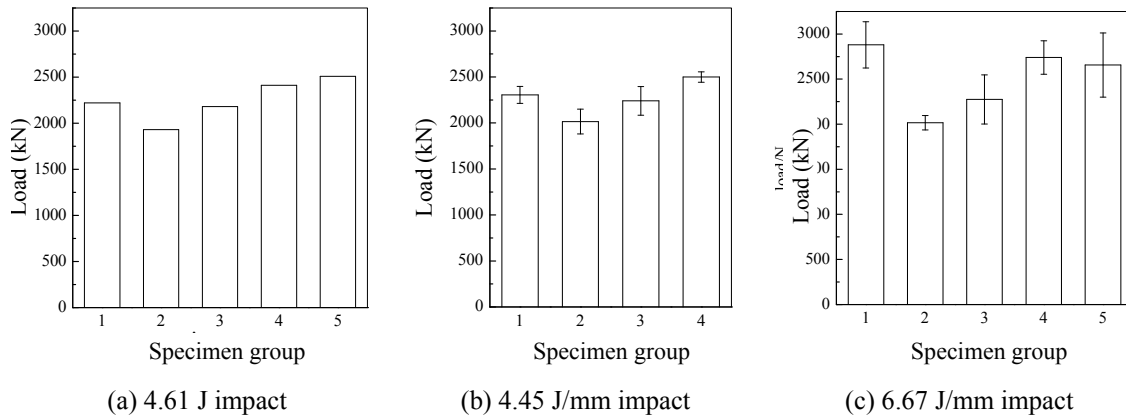


Fig. 9 DTLs of each group specimens under three different impact energy level

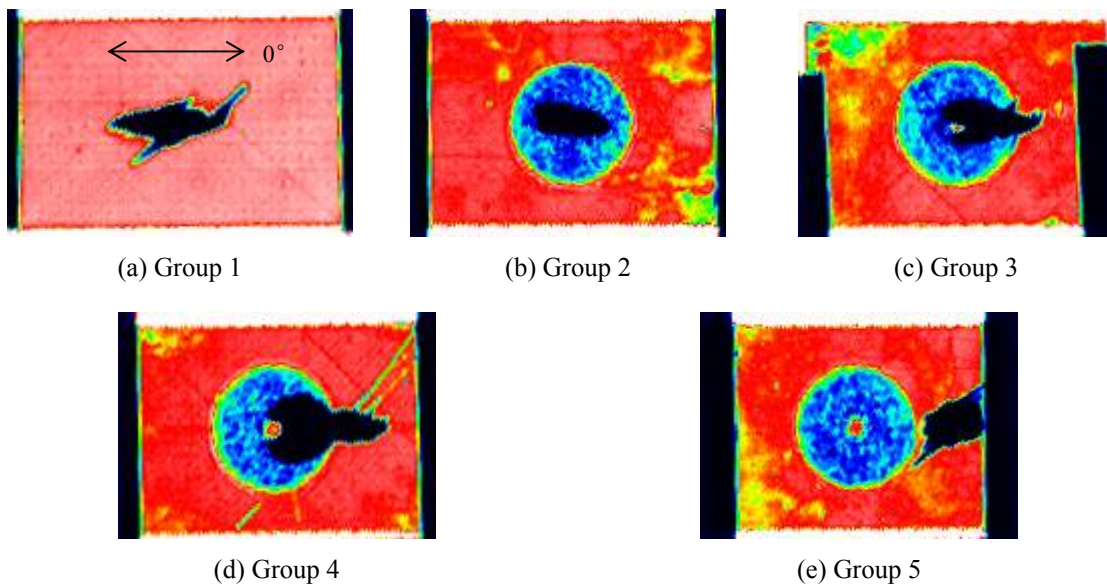


Fig. 10 Ultra C-scan images of five group specimens after 6.67 J/mm impact

5. Low-velocity impact damage

To detect the internal damage in the repaired laminates, ultra C-scan is used to detect the shape and area of the damaged zone. To further characterize the damage, several of coupons are sectioned through the center of the damaged area. And the laminates used to analyze the impact damage here are all subjected to 6.67 J/mm.

5.1 Ultra C-scan inspection

Figs. 10(a)-(e) show the typical ultra C-scan images of impact damage of five group specimens.

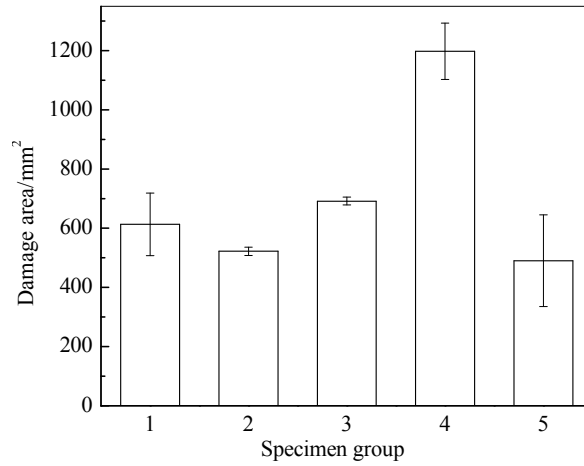


Fig. 11 Projection damage areas of five group specimens after 6.67 J/mm impact

Fig. 10(a) shows the damage of an original laminate after impact, the projection of damage seems to be long and thin, and its longitudinal direction parallels to the fiber direction of the first ply. Figs. 10(b)-(e) are the ultra C-scan images of repaired laminates after impact at P2, P3, P4 and P5 respectively. It can be found that the damage area is much larger when the repaired laminate is impacted at P3, the bond line of the top surface. While the damage zone is restricted to the patch when impacted at the center of the patch and to the parent laminated when impacted at 15 mm away from the bond line.

The projection damage areas of the five group specimens are shown in Fig. 11.

5.2 Microscopic examination of the laminate damage near impact point

Samples for the micrographic analysis for the repaired composite laminates subjected to 6.67 J/mm impact are cut from the repaired specimens with impact damage, and the region is located at the impact point, as is shown in Fig. 12 in which the view direction is represented by the arrow.

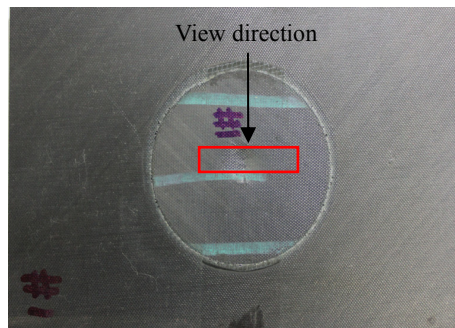


Fig. 12 The location of the sample taken from the repaired specimen for microscopic examination and its view direction

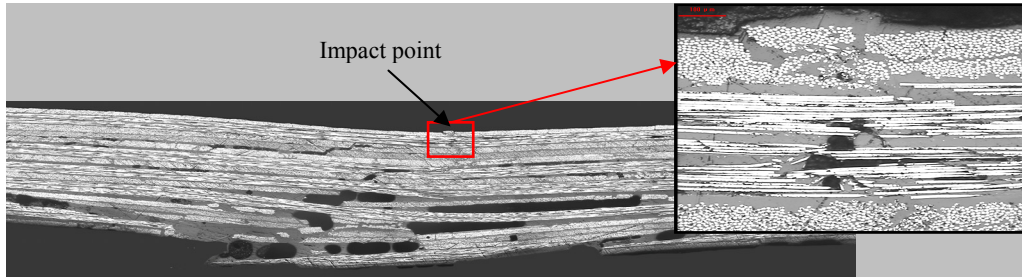


Fig. 13 Micrograph of the repaired laminate subjected to impact at P1

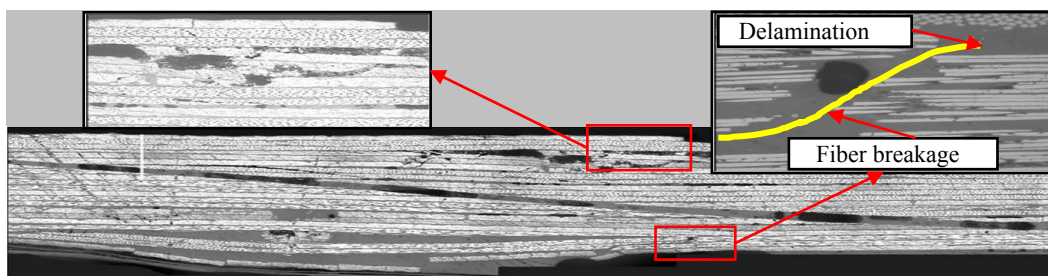


Fig. 14 Micrograph of the repaired laminate subjected to impact at P2

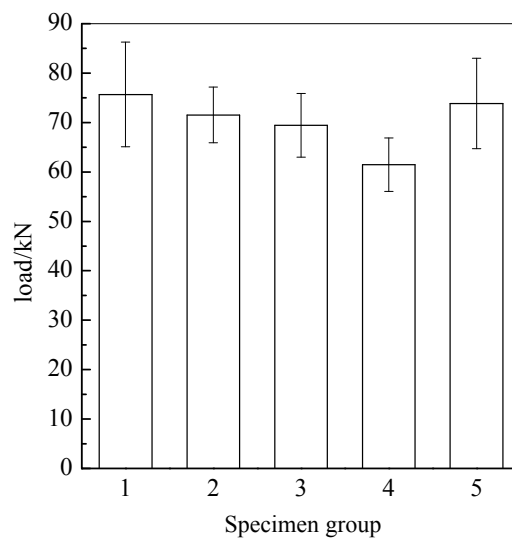


Fig. 15 CAI strength of the five group specimens subjected to 6.67 J/mm impact

The longitudinal sectional view is observed using a UHL VMM200 micro-scope with a magnification of 100 and can produced an optical resolution from point to point of 1 μm precision.

As is shown in Fig. 13, there are numerous matrix crack, fiber breakage and delamination in the patch when the impact position is located at P1, the center of the patch top surface. While there is

no obvious matrix crack and delamination in the parent laminate, and the bond between the patch and the parent laminate remains intact. On the other hand, once the impact location transfers to P2, there are obvious matrix cracks and delamination in both the patch and parent laminate, as is shown in Fig. 14. Moreover, a lot of fiber flexures and matrix cracks are observed in the back of parent laminate, where the delamination is more obvious and the damaged area is larger.

6. CAI strength

The CAI strength of the five group specimens subjected to 4.45 J/mm impact and their scatters are shown in Fig. 15.

In the column graph, horizontal coordinate represents for the group number and the vertical coordinate represents for the residual compression strength. Group 1 and Group 5 results indicate that the CAI of the repaired laminate subjected to impact at the parent laminate is almost the same with that of the original laminate. Comparing Group 2, Group 3 and Group 4, a slight decrease of CAI strength can be found when the impact location transfers from P2 to P4. Furthermore, there is a good negative correlation between the residual compressive strength and the projection damage area. When the damage area is larger, the CAI tends to be smaller.

7. Conclusions

Repaired composite laminates are also faced with the threat of low-velocity impact. Due to the present of the patch, the impact location will exert certain influence on laminate impact damage. Based on the experimental study of scarf-repaired CCF300/5228A laminates subjected to a low-velocity impact, by conduction damage detection and subsequent compression tests, the following conclusions can be concluded:

- The contact load history of the repaired laminate differs from that of the original laminate when subjected to a low-velocity impact. For scarf repaired laminates, the impact location exerts specific influence on the load response.
- The impact location can affect the delamination threshold load of the scarf-repaired laminate. The lowest delamination threshold load is gained when the repaired laminate is impacted at the patch center, indicating that the structure is more vulnerable to delamination when subjected to an impact at this location.
- When the impact is imposed on the region that contains the repair bonding interface in the thickness direction, debonding will be generated on the interface between the adhesive layer and the composite laminates. The closer the impact point is to the bonding line, the larger the debonding area will be.
- In general, laminate CAI strength reduces after it is scarf-repaired. For scarf-repaired laminates, the CAI strength varies when impacted at different locations. The repaired laminates with debonding have lower CAI strength, and the CAI strength is much lower when it carries a larger debonding area.
- When the scarf-repaired laminate is impacted at the location away from the patch edge, its contact load history, delamination threshold load and CAI strength are all similar than those of original laminates. That means the influence of scarf-repair on the parent lamiante can be ignored.

References

- Abrate, S. (1991), "Impact on laminated composite materials", *Appl. Mech. Rev.*, **44**(4), 155-190.
- Abrate, S. (1994), "Impact on laminated composites: recent advances", *Appl. Mech. Rev.*, **47**(11), 517-544.
- ASTM D7136/D7136M-07 (2007), "Measuring the damage resistance of a fiber-reinforced polymer matrix composite to a drop-weight impact event", *American Society for Testing Materials*.
- ASTM D7137/D7137M-07 (2007), "Compressive residual strength properties of damaged polymer matrix composite plates", *American Society for Testing Materials*.
- Baker, A.A. (1999), "Scarf repairs to highly strained graphite/epoxy structure", *Int. J. Adhes. Adhes.*, **19**(2), 161-171.
- Cheng, X.Q., Kou, C.H. and Li, Z.N. (1998), "Compression of composite honeycomb core sandwich panels after low velocity impact", *J. Beijing Univ. Aeron. Astron.*, **24**(5), 551-554.
- Cheng, X.Q., Zhang, Z.L. and Wu, X.R. (2002), "Post-impact compressive strength of small composite laminate specimens", *Acta Materiae Compositae Sinica*, **19**(6), 8-12.
- Cheng, X.Q., Ali, A.M. and Li, Z.N. (2009), "Residual strength of stitched laminates after low velocity impact", *J. Reinf. Plast. Compos.*, **28**(14), 1670-1688.
- Falzon, B.G. (2009), "Impact damage and repair of composite structures", *Aeronaut. J.*, **113**(1145), 431-445.
- Harman, A.B. (2006), "Optimisation and improvement of the design of scarf repairs to aircraft", Ph.D. Dissertation, University of New South Wales, Sydney, Australia.
- Harman, A.B. and Rider, A.N. (2011), "Impact damage tolerance of composite repairs to highly-loaded, high temperature composite structures", *Compos. Part A – Appl. S. Manuf.*, **42**(10), 1321-1334.
- Harman, A.B. and Wang, C.H. (2007), "Damage tolerance and impact resistance of composite scarf joints", *Proceedings of the 16th International Conference on Composite Materials (ICCM-16)*, Kyoto, Japan, July.
- Herszberg, I., Feih, S., Gunnion, A.J. and Li, H.C. (2007), "Impact damage tolerance of tension loaded bonded scarf repairs to CFRP laminates", *Proceedings of the 16th International Conference on Composite Materials (ICCM-16)*, Tokyo, Japan, July.
- Hoshi, H., Nakano, K. and Iwahori, Y. (2007), "Study on repair of CFRP laminates for aircraft structures", *Proceedings of the 16th International Conference on Composite Materials (ICCM-16)*, Tokyo, Japan, July.
- Kumar, S.B., Sivashanker, S., Bag, A. and Sridhar, I. (2005), "Failure of aerospace composite scarf-joints subjected to uniaxial compression", *Mater. Sci. Eng.: A*, **412**(1), 117-122.
- Kumar, S.B., Sridhar, I., Sivashanker, S., Osiyemi, S.O. and Bag, A. (2006), "Tensile failure of adhesively bonded CFRP composite scarf joints", *Mater. Sci. Eng.: B*, **132**(1), 113-120.
- Schoeppner, G.A. and Abrate, S. (2000), "Delamination threshold loads for low velocity impact on composite laminates", *Compos. Part A – Appl. S. Manuf.*, **31**(9), 903-915.
- Takahashi, I., Ito, Y., Takeda, S., Iwahori, Y., Takatsubo, J. and Takeda, N. (2007), "Impact damage detection on scarf-repaired composites using Lamb wave sensing", *Proceedings of the 16th International Conference on Materials (ICCM-16)*, Kyoto, Japan, July.
- Wang, C.H. and Gunnion, A.J. (2008), "On the design methodology of scarf repairs to composite laminates", *Compos. Sci. Technol.*, **68**(1), 35-46.